OPEN

The ISME Journal (2015), 1–13

www.nature.com/ismej

ORIGINAL ARTICLE

Microbial carbon metabolism associated with electrogenic sulphur oxidation in coastal sediments

Diana Vasquez-Cardenas[1,2], Jack van de Vossenberg[2,6], Lubos Polerecky[3], Sairah Y Malkin[4,7], Regina Schauer[5], Silvia Hidalgo-Martinez[2], Veronique Confurius[1], Jack J Middelburg[3], Filip JR Meysman[2,4] and Henricus TS Boschker[1]

[1]*Department of Marine Microbiology, Royal Netherlands Institute for Sea Research (NIOZ), Yerseke, The Netherlands;* [2]*Department of Ecosystem Studies, Royal Netherlands Institute for Sea Research (NIOZ), Yerseke, The Netherlands;* [3]*Department of Earth Sciences, Utrecht University, Utrecht, The Netherlands;* [4]*Department of Environmental, Analytical and Geo-Chemistry, Vrije Universiteit Brussel (VUB), Brussels, Belgium and* [5]*Centre of Geomicrobiology/Microbiology, Department of Bioscience, Aarhus University, Aarhus, Denmark*

Recently, a novel electrogenic type of sulphur oxidation was documented in marine sediments, whereby filamentous cable bacteria (Desulfobulbaceae) are mediating electron transport over cm-scale distances. These cable bacteria are capable of developing an extensive network within days, implying a highly efficient carbon acquisition strategy. Presently, the carbon metabolism of cable bacteria is unknown, and hence we adopted a multidisciplinary approach to study the carbon substrate utilization of both cable bacteria and associated microbial community in sediment incubations. Fluorescence *in situ* hybridization showed rapid downward growth of cable bacteria, concomitant with high rates of electrogenic sulphur oxidation, as quantified by microelectrode profiling. We studied heterotrophy and autotrophy by following ^{13}C-propionate and -bicarbonate incorporation into bacterial fatty acids. This biomarker analysis showed that propionate uptake was limited to fatty acid signatures typical for the genus *Desulfobulbus*. The nanoscale secondary ion mass spectrometry analysis confirmed heterotrophic rather than autotrophic growth of cable bacteria. Still, high bicarbonate uptake was observed in concert with the development of cable bacteria. Clone libraries of 16S complementary DNA showed numerous sequences associated to chemoautotrophic sulphur-oxidizing Epsilon- and Gammaproteobacteria, whereas ^{13}C-bicarbonate biomarker labelling suggested that these sulphur-oxidizing bacteria were active far below the oxygen penetration. A targeted manipulation experiment demonstrated that chemoautotrophic carbon fixation was tightly linked to the heterotrophic activity of the cable bacteria down to cm depth. Overall, the results suggest that electrogenic sulphur oxidation is performed by a microbial consortium, consisting of chemoorganotrophic cable bacteria and chemolithoautotrophic Epsilon- and Gammaproteobacteria. The metabolic linkage between these two groups is presently unknown and needs further study.

The ISME Journal advance online publication, 13 February 2015; doi:10.1038/ismej.2015.10

Introduction

The traditional view of diffusion-controlled redox zonation in marine sediments has recently been challenged by the observation that microorganisms are capable of transporting electrons over cm-scale distances (Nielsen *et al.,* 2010). This long-distance electron transport is mediated by filamentous cable bacteria belonging to the Desulfobulbaceae that are proposed to catalyse a new electrogenic form of sulphur oxidation (Pfeffer *et al.,* 2012). Cable bacteria have recently been found in a wide range of marine sediment environments (Malkin *et al.,* 2014), and seem to be competitively successful, because they can harvest electron donors (sulphide) at cm depth in the sediment while still utilizing thermodynamically favourable electron acceptors such as oxygen and nitrate (Nielsen *et al.,* 2010; Marzocchi *et al.,* 2014) that are only available in the first mm of coastal sediments.

The current conceptual model of electrogenic sulphur oxidation (e-SOx) envisions a new type of metabolic cooperation between cells, where

Correspondence: D Vasquez-Cardenas, Department of Marine Microbiology, Royal Netherlands Institute for Sea Research (NIOZ), Korringaweg 7, 4401 NT Yerseke, The Netherlands.
E-mail: diana.vasquez@nioz.nl
[6]Current address: UNESCO-IHE, Delft, The Netherlands.
[7]Current address: Marine Sciences Department, University of Georgia at Athens (UGA), Athens, GA, USA.
Received 24 September 2014; revised 8 December 2014; accepted 16 December 2014

different cells from the same multicellular filament perform distinct redox half reactions. Anodic cells located in suboxic and anoxic sediment zones obtain electrons from sulphide and liberate protons (anodic half-reaction: $\frac{1}{2}\,H_2S + 2H_2O \rightarrow \frac{1}{2}\,SO_4^{2-} + 4e^- + 5H^+$). These electrons are then transported along the longitudinal axis of the filament to cells located near the sediment–water interface (Pfeffer *et al.,* 2012). At the thin oxic layer near the sediment surface, cathodic cells reduce oxygen and consume protons (cathodic half-reaction: $O_2 + 4e^- + 4H^+ \rightarrow 2H_2O$). The two half-reactions leave a distinct geochemical fingerprint in the sediment consisting of a shallow oxygen penetration depth, a cm-wide suboxic zone separating the oxic and sulphidic sediment horizons, and a characteristic pH depth profile, defined by a sharp pH maximum within the oxic zone and a deep and broader pH minimum at the bottom of the suboxic zone (Nielsen *et al.,* 2010).

Laboratory time-series experiments (Malkin *et al.,* 2014; Schauer *et al.,* 2014) show that a network of cable bacteria can rapidly (<10 days) develop in sediments, reaching high filament densities (>2000 m of filaments per cm^{-2} after 21 days; Schauer *et al.,* 2014) with fast generation times of ~20 h. Furthermore, the progressive downward growth of the cable bacteria closely correlates with the widening of the suboxic zone and a strong increase in biogeochemical rates, such as sedimentary oxygen consumption (Malkin *et al.,* 2014; Schauer *et al.,* 2014). One could hypothesize that cable bacteria may have a similar metabolism to their closest cultured relative *Desulfobulbus propionicus* (Pfeffer *et al.,* 2012) that can efficiently grow as a chemoorganotroph in propionate-rich media while obtaining metabolic energy from oxidation of sulphide to elemental sulphur followed by sulphur disproportionation (Widdel and Pfennig, 1982; Dannenberg *et al.,* 1992; Fuseler and Cypionka, 1995; Pagani *et al.,* 2011). It is presently unclear whether they are organotrophs (heterotrophs) or lithoautotrophs (chemoautotrophs).

Here, we adopted a multidisciplinary approach to characterize the carbon metabolism in coastal sediments with e-SOx activity, resolving the carbon substrate uptake of both cable bacteria and their associated microbial community. We conducted a series of laboratory incubations, starting in March 2012, to track the temporal development of the cable bacteria network by microsensor profiling and fluorescence *in situ* hybridization (FISH), and quantified inorganic carbon fixation at various time points through biomarker analysis of phospholipid-derived fatty acids combined with stable-isotope probing (PLFA-SIP). In August 2012, we studied both inorganic carbon and propionate uptake by PLFA-SIP. In both months, we examined the linkage between carbon metabolisms and e-SOx activity through targeted manipulation treatments. The active microbial community in the March and August experiments was characterized by 16S complementary DNA (cDNA) clone libraries. The final experiment in May 2013 quantified the carbon tracer uptake of both inorganic (bicarbonate) and organic (propionate) substrates by individual cable bacteria filaments using nanoscale secondary ion mass spectrometry (nanoSIMS).

Materials and methods

Sediment collection and incubation

Sediment was collected from a seasonally hypoxic coastal basin (Marine Lake Grevelingen, The Netherlands; 51°44'50.04"N, 3°53'24.06"E; water depth 32 m) using a gravity corer (UWITEC, Mondsee, Austria). At the sampling site, e-SOx activity and associated cable bacteria were previously documented under field conditions (Malkin *et al.,* 2014). The top 20 cm of the sediment was collected, homogenized and repacked into poly(methyl methacrylate) acrylic cores (15 cm height; 4 cm inner diameter). Sediment cores were subsequently incubated at 16 °C (±1) in a darkened incubation tank with filtered (0.2 μm) sea water (salinity 30). During incubations, the overlying water was kept at 100% air saturation by continuous air bubbling. Three sediment incubation experiments were conducted: in March 2012, we documented the bacterial community structure and substrate utilization during the temporal development of e-SOx and performed initial targeted manipulation experiments; in August 2012, we performed targeted manipulation experiments on cores in which e-SOx had established; and finally in May 2013, we picked individual cable bacteria filaments from sediments with e-SOx for nanoSIMS analysis after stable isotope labelling.

Microsensor profiling

Microsensor profiling (O_2, pH, H_2S) was performed as described in Malkin *et al.* (2014) to determine the geochemical fingerprint of the e-SOx process, and hence the developmental state of e-SOx in the incubated sediments. One set of microsensor profiles was taken per core and 3 to 6 replicate cores were analysed per time point (March: days 1, 2, 3, 6, 8, 9, 10 and 13, August: day 12; May: day 20). Two biogeochemical rates were calculated from microsensor profiles: the total diffusive oxygen uptake (DOU) of the sediment that provides a proxy for the activity of the whole microbial community, and the cathodic oxygen consumption (COC) that is the part of the DOU that can be attributed to the cathodic half-reaction of e-SOx and that reflects the activity of the cable bacteria (details on calculation are given in Supplementary Information).

PLFA-SIP analysis

Biomarker analysis of PLFA-SIP allows linking bacterial identity and activity (Boschker *et al.,*

1998). In the March and August 2012 experiments, carbon incorporation was assessed by addition of ^{13}C-bicarbonate and ^{13}C-propionate. Stock solutions of 20 mM of ^{13}C-bicarbonate and 1.7 mM of ^{13}C-propionate (both 99% ^{13}C; Cambridge Isotope Laboratories, Andover, MA, USA) were prepared in calcium- and magnesium-free artificial sea water to prevent carbonate precipitation and bubbled with nitrogen gas shortly before use to remove oxygen.

In the March experiment, only ^{13}C-bicarbonate was used as substrate, and additions were performed after 1, 9 and 13 days. In the August experiment, both ^{13}C-bicarbonate and ^{13}C-propionate were used as substrates (addition at day 12 of incubation). All labelling experiments were conducted in duplicate cores. ^{13}C-carbon substrates were added to the sediment cores with the line injection method (Jørgensen, 1978), adding label via vertically aligned side ports in the core liners. For further details on injections and incubation setup see Supplementary Information. After 24 h of incubation with labelled substrate, cores were sectioned in four layers: 0–0.3 cm, 0.3–0.8 cm, 0.8–1.5 cm and 1.5–3.0 cm.

Biomarker extractions were performed on freeze dried sediment as in Guckert *et al.* (1985) and Boschker *et al.* (1998) and ^{13}C-incorporation into PLFA was analysed by gas chromatography–isotope ratio mass spectrometry (Thermo, Bremen, Germany) on an apolar analytical column (ZB5-MS Phenomenex, Utrecht, Netherlands). Label incorporation was calculated from the product of the concentration of each fatty acid and the increase in ^{13}C abundance relative to the background ^{13}C abundance (Boschker and Middelburg, 2002). Total carbon incorporation with propionate and bicarbonate was corrected for dilution of ^{13}C-substrates in pore water (see Supplementary Information for details). Bacterial PLFA (12:0 to 20:0) were summed and converted to biomass production assuming an average PLFA carbon contribution of 5.5% of total bacterial carbon (Brinch-Iversen and King, 1990; Middelburg *et al.,* 2000).

To determine which biomarkers characterize the bicarbonate- and propionate-consuming bacterial communities in the sediment, we performed principal component analysis using R free statistical software (Vienna, Austria) (prcomp{stats} module). PLFA incorporation data (pmol C per g dry weight) were first normalized to total ^{13}C incorporation and then $\log(x+1)$ transformed. Samples for principal component analysis were selected based on the presence of filaments (minimum 100 m of cable bacteria cm^{-3}), and sufficient ^{13}C-mol incorporation in fatty acids (only samples with $>1\%$ of the total sediment activity were included).

Nanoscale secondary ion mass spectrometry

In the May 2013 experiment, microsensor profiling showed that the e-SOx process was fully established 21 days after the start of the incubation. NanoSIMS analysis was used to visualize and quantify ^{13}C-bicarbonate and ^{13}C-propionate uptake by individual cells within cable bacteria filaments. Stock solutions of ^{13}C-labelled substrate were prepared as for PLFA-SIP, but with higher label concentrations (bicarbonate, 62 mM; propionate, 11 mM), given the lower ^{13}C-sensitivity of the nanoSIMS technique. In total, 500 µl was injected using the line injection method, starting from 5 cm depth up to the sediment surface (10 parallel injections in a 1 cm^2 area). Sediment cores were subsequently incubated for 24 h in the dark at 16 °C. Core sectioning depths were based on microsensor profiling results: a first slice contained the oxic zone (0 to 0.2 cm) and a second slice spanned the suboxic zone (0.4 to 2.0 cm). Individual filaments were picked under a microscope with fine glass hooks made from Pasteur pipettes, and washed several times in artificial sea water to remove sediment particles with a final wash in milliQ (Millipore, Amsterdam, Netherlands) to eliminate salt. Isolated filaments were subsequently transferred to gold-sputtered glass slides (0.5 cm diameter, 10 nm gold coating), and dried in a desiccator before analysis. Filaments from the sulphidic layer were not included in the study given that not enough filaments could be collected from below 2.0 cm in all treatments. Filaments were retrieved in a similar manner from cores without label addition and served as controls.

NanoSIMS analysis was performed with a nanoSIMS 50L instrument (Cameca, Paris, France) at Utrecht University, Utrecht, The Netherlands) as described in the Supplementary Information. The counts of ^{12}C and ^{13}C from individual filaments were measured and used to calculate the relative ^{13}C fraction as $^{13}C/(^{12}C+^{13}C)$. Overall, between 3 and 6 different filaments were analysed from each sample, consisting in total of 39 cells for natural ^{13}C-abundance Controls (oxic zone), 75 cells for ^{13}C-propionate uptake (oxic and suboxic zones) and 53 cells for ^{13}C-bicarbonate label uptake (oxic and suboxic zones). For further calculation of C uptake, the average relative ^{13}C abundance of the treated filaments were subtracted from those of the Controls and for final concentrations of ^{13}C-labelled substrates in pore water, as mentioned above for the PLFA-SIP analysis. Abundance of cable bacteria from FISH counts was used to convert ^{13}C enrichment to carbon incorporation rates. Differences in initial ^{13}C-label substrate concentrations and volume of ^{13}C-labelled substrate injected into the sediment were taken into account to compare carbon uptake rates estimated from nanoSIMS results with those obtained from PLFA-SIP analysis.

Manipulation experiments

To further investigate the relationship between e-SOx activity and carbon metabolism, we conducted two types of sediment manipulations in

combination with the two ^{13}C-labelled substrates for PLFA-SIP analysis for both the March and August experiments. For the first manipulation we induced anoxia by depleting the overlying water of oxygen, thus impeding all forms of aerobic sulphide oxidation, including e-SOx (Nielsen *et al.,* 2010). The second treatment involved a horizontal cutting of the sediment with a thin nylon thread (60 μm diameter) that selectively disrupts the e-SOx process by interrupting electron transport by the cable bacteria (Pfeffer *et al.,* 2012). We used two cutting depths: a shallow cut below the oxic zone at 0.3 cm depth and deeper cut in the middle of the suboxic zone at 0.8 cm (see Table 1 for experimental setup). All cores were microprofiled before the experiment and only those cores that showed an e-SOx signature were selected for manipulation. Substrate injections were done as for PLFA-SIP analysis. All treatments were done in duplicate cores.

For the anoxic treatment, cores were incubated in nitrogen bubbled overlying water. Cutting was done by fixing a ring on top of the core liner with a height equivalent to the cutting depth. The sediment was subsequently pushed up slowly with a plunger until the top of the ring. Once the sediment was in place, a nylon thread was passed through the sediment guided by the slit between the core liner and the ring, and the slit was later sealed with water-proof adhesive tape. Sediment cores with <1 day of incubation were used as control sediment (that is, without e-SOx). These controls were examined 1 to 3 h after the cut as well as 24 h after manipulation, showing that cutting treatment had no effect on microsensor profiles (Supplementary Figure S1).

Fluorescence in situ hybridization

The depth distribution of cable bacteria was quantified via FISH analysis performed on one sediment core for each of the three time points in March and at the end of the incubation in August. Sediment cores were sliced in the same four layers as described for PLFA-SIP. The FISH procedure was according to Schauer *et al.* (2014) with probe DSB706 (Manz *et al.,* 1992).

At each time point the total filament length per unit of sediment volume ($m\,cm^{-3}$) was calculated (Schauer *et al.,* 2014) as well as the areal density of cable bacteria ($m\,cm^{-2}$) by depth integration over all four sediment layers. Number of cells, 3 μm in length, was estimated from filaments lengths and converted to biovolume (μm^3) with measured cell diameter. Biovolume was then converted to carbon biomass by adopting the allometric scaling formula $B = 435\ V^{0.86}$ ($B = fg\ C\ \mu m^{-3}$; $V = \mu m^3$, Romanova and Sazhina, 2010) assuming a cylindrical cell shape and a carbon content equal to 50% of the dry weight.

16S cDNA libraries

To describe the active community composition, 16S cDNA clone libraries were constructed per sediment layer at day 13 March (354 clones total) and day 12 August (301 clones total). Methods and data analysis were as described in Malkin *et al.* (2014), where 16S cDNA was amplified by PCR using general bacterial primers Bac F968 (5′-AACGCGAAGAACCTTAC-3′) and Bac R1401 (5′-CGGTGTGTACAAGRCCCGGG AACG-3′). Sequences have been submitted to GenBank database under accession no BankIt1781572: KP265396–KP265657.

Results

Development of electrogenic sulphur oxidation

On day 1 of the March experiment, there was no suboxic zone present with sulphide accumulating right below the mm deep oxygen penetration. The geochemical fingerprint of e-SOx became apparent after 6 days (not shown), and by day 9, there was a pronounced subsurface pH maximum and a $\sim$5 mm wide separation between the O_2 and H_2S horizons, indicative of developing e-SOx activity (Figure 1a). This suboxic zone progressively widened over the following days (Figure 1a), reaching a width of $\sim$15 mm at day 13. In August, the sediment biogeochemistry showed a very similar development, showing a $\sim$18 mm wide suboxic zone accompanied by the typical subsurface pH maximum after 12 days of incubation.

Table 1 Total inorganic carbon and propionate incorporation rates calculated from PLFA-SIP analysis from the top 3 cm

Date		*Treatment*	*Cable bacteria biomass (mmol C m^{-2})*	*Propionate incorporation (mmol C m^{-2} day^{-1})*	*Inorganic carbon incorporation (mmol C m^{-2} day^{-1})*	*DOU (mmol O_2 m^{-2} day^{-1})*
March	1	Control	6	NA	1.6 ± 0.5	51 ± 4
	9	Control	130	NA	9.6 ± 2.4	45 ± 3
	13	Control	166	NA	10.9 ± 0.9	76 ± 4
		Anoxic	NA	NA	0.5 ± 0.1	NA
		0.3 cm cut	NA	NA	7.3 ± 0.5	64 ± 15
August	12	Control	229	16.7 ± 3.7	7.3 ± 2.2	78 ± 18
		Anoxic	NA	2.0 ± 0.2	NA	NA
		0.3 cm cut	NA	9.7 ± 5.7	6.5 ± 1.9	57 ± 23
		0.8 cm cut	NA	9.4 ± 0.9	6.0 ± 1.9	28 ± 6

Abbreviations: DOU, dissolved oxygen uptake; NA, not analysed; PLFA-SIP, phospholipid-derived fatty acids combined with stable-isotope probing.
DOU was calculated from microsensor profiles. Averages (± s.d.) are listed.

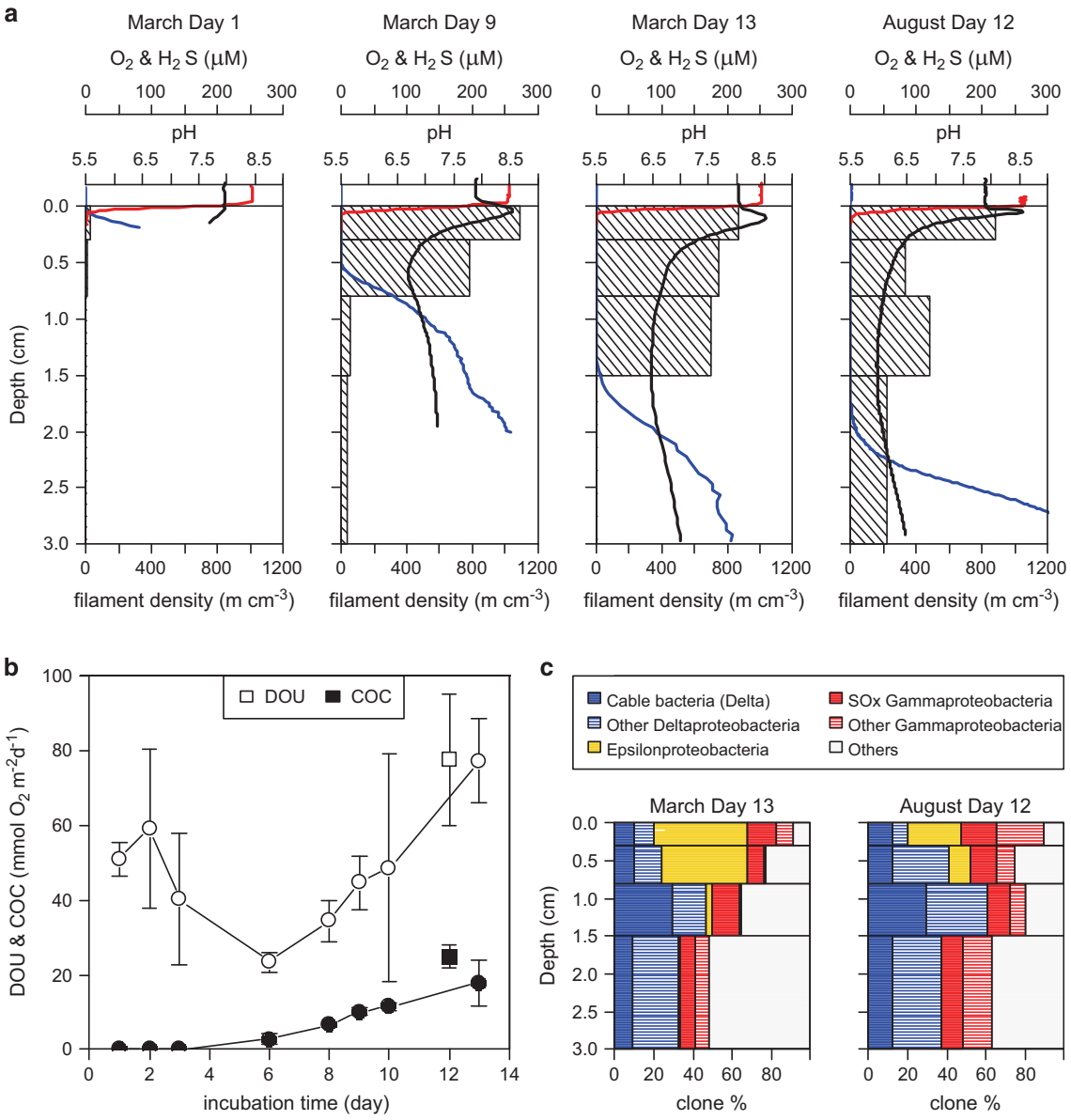

Figure 1 Development of e-SOx and abundance of the associated cable bacteria. (**a**) Microsensor profiles (H_2S, O_2, pH) that show the geochemical e-SOx signature and the density of cable bacteria (bars). (**b**) Temporal variation of DOU and COC calculated from the microsensor profiles. Circles represent data from March 2012 experiment, whereas squares indicate values for the August 2012 incubation. (**c**) Relative contribution of 16S cDNA sequences related to cable bacteria and other main phylogenic groups for sediment with strong e-SOx signal (day 13 March and day 12 August). In the legend, SOx stands for sulphur-oxidizing bacteria. A detailed phylogenetic tree of all operational taxonomic units (OTUs) is included in Supplementary Figure S2.

FISH counts for March showed that cable bacteria progressively grew from the sediment surface towards the deeper layers in unison with the widening of the suboxic zone (Figure 1a). Depth integrated filament length increased 90-fold from day 1 (13 m cm^{-2}) to day 13 (1131 m cm^{-2}), providing a final cable biomass of 166 mmol C m^{-2} (Table 1). The mean biomass accumulation rate over the whole 13-day experiment amounted to 13 mmol C m^{-2} day^{-1}. The filament density at the end of the August experiment reached 1095 m cm^{-2} with a corresponding biomass of 229 mmol C m^{-2}, resulting in a mean biomass accumulation rate of 19 mmol C m^{-2} day^{-1}. For both experiments, filament diameter progressively increased downwards in the oxic zone 0.97 ± 0.10 μm, in the suboxic zone 1.23 ± 0.17 μm and in the sulphidic zone 1.47 ± 0.22 μm.

Over the first 6 days of the March experiment, the DOU of the sediment gradually decreased (Figure 1b). This has been previously observed in similar incubations, and was attributed to transient oxidation of reduced compounds initially present in the top of the homogenized sediment (Malkin *et al.,* 2014; Schauer *et al.,* 2014). After day 6, when the e-SOx signature became first visible, the DOU

increased steeply, reaching a maximum value of 80 mmol m^{-2} day^{-1} on day 13 (Figure 1b and Table 1). The COC, as derived from the alkalinity balance calculations (see Supplementary Information), represented 13% of the total DOU on day 6 and reached a maximum of 32% by day 13. However, the observed increase in DOU between days 6 and 13 was much higher (54 mmol m^{-2} day^{-1}), accounting for 70% of the DOU at day 13. This higher contribution of e-SOx to the overall oxygen consumption is consistent with subsequent manipulation experiments (see below) suggesting that the alkalinity balance procedure may underestimate the true COC.

Microbial community structure

Clone libraries of 16S cDNA from both the March and August incubations revealed three main classes known to be involved in sulphur cycling. Deltaproteobacteria sequences constituted the first class (35% of total clones), of which on average 45% were highly similar (>97% sequence identity) to previously reported sequences for cable bacteria (Supplementary Figure S2). Cable bacteria sequences were found up to 3 cm depth (Figure 1c) and formed two operational taxonomic units each dominated by sequences from the two different experiments (Supplementary Figure S2). The second predominant clade (21% of total clones) was composed of Gammaproteobacteria that were present throughout the sediment (March 56 clones and August 82 clones, Figure 1c), and of which 40% were closely related to chemoautotrophic sulphur oxidizers (candidatus *Parabeggiatoa communis*, *Thiomicrospira frisia* and *T. halophile*) in addition to chemoautotrophic endosymbionts of bivalves, oligochaetes and ciliates (Supplementary Figure S2). The third class (17% of total clones) contained chemoautotrophic sulphur-oxidizing Epsilonproteobacteria from the *Sulfurimonas*, *Sulforovum* and *Arcobacter* genera (Supplementary Figure S2). These clones were present in the top 1.5 cm of sediment in March and top 0.8 cm in August sediment (Figure 1c). The remaining sequences (27%) belonged to a variety of phylogenetic groups related to Verrucomicrobia, Nitrospirae, candidate division OP8, Planctomycetes and some Cyanobacteria.

Carbon isotope labelling

PLFA-SIP analysis revealed a clear distinction between bicarbonate- and propionate-consuming bacterial populations (Figure 2). Biomarker fingerprints from the inorganic carbon-assimilating community were similar to those of sulphur-oxidizing Gamma- and Epsilonproteobacteria (Figure 2a; Inagaki *et al.,* 2004; Donachie *et al.,* 2005; Zhang *et al.,* 2005; Takai *et al.,* 2006), characterized by ^{13}C-uptake in 16:1ω7c, 16:0, 14:0, 18:1ω7c and 16:1ω5c PLFA. In contrast, propionate incorporation was differentiated by high ^{13}C labelling in 17:1ω6c, 15:0, 16:1ω7c and 17:1ω8c that resemble the PLFA fingerprint of the genus *Desulfobulbus* spp. (Figure 2b). Depth integrated carbon incorporation rates for each substrate are listed in Table 1.

NanoSIMS analysis confirmed the preferential uptake of ^{13}C-propionate over ^{13}C-bicarbonate by individual cable bacteria filaments (Figure 3). Depth integrated carbon incorporation rate determined by nanoSIMS, combined with filament densities determined by FISH (oxic: 10 μmol C cm^{-3} and suboxic: 18 μmol cm^{-3}) show that ^{13}C-enrichment in filaments for ^{13}C-bicarbonate incubations was only ~20% of ^{13}C-enrichment with ^{13}C-propionate. Carbon uptake rates yielded a doubling time of filament biomass for propionate (20 h) that was 3.5 times faster than for bicarbonate (71 h), suggesting cable bacteria cannot maintain rapid growth on an autotrophic metabolism. Carbon uptake rates of 7 mmol m^{-2} day^{-1} for propionate and 2 mmol m^{-2} day^{-1} for bicarbonate were comparable to the depth integrated rates for the propionate- and bicarbonate-consuming bacterial communities obtained with PLFA-SIP (Table 1). Interestingly, incorporation of ^{13}C-propionate by filaments in surface sediment was higher and more homogenous among cells (Figure 3b) than in deeper sediment horizons where some filaments showed little ^{13}C-enrichment whereas others had high ^{13}C-enrichment (Figure 3e).

Experiments revealed substantial rates of organic and inorganic carbon assimilation that extended to cm depth into the sediment (Figure 4). Remarkably, in March bicarbonate uptake expanded in synchrony with the development of the cable bacteria network and the deepening of the sulphide horizon (Figures 4a–c), resulting in an almost even distribution throughout the oxic and suboxic zones by day 13 (Figures 4a–c). In August (day 12), inorganic carbon fixation was also present down to 3 cm deep, but the maximum activity was found in the oxic zone (Figure 4d). Propionate uptake was highest in the top mm and extended below the sulphide horizon (Figure 4e).

Targeted manipulation experiments

Manipulation experiments had clear effects on the geochemical fingerprint, and the carbon uptake rates (Figure 5). In the anoxic treatment the characteristic subsurface pH peak decreased from 8.4 to 7.7 after 24 h of incubation, indicating a strong decline in cathodic proton consumption (Figure 5a). In parallel, both inorganic and organic carbon uptake were almost completely inhibited throughout the sediment (Figures 5d and g), demonstrating that most of the microbial activity in the suboxic and sulphidic zones was linked to the presence of oxygen at the sediment surface.

Shallow cutting of the sediment (0.3 cm depth) induced an immediate geochemical response: within 1 h, the pH maximum decreased from

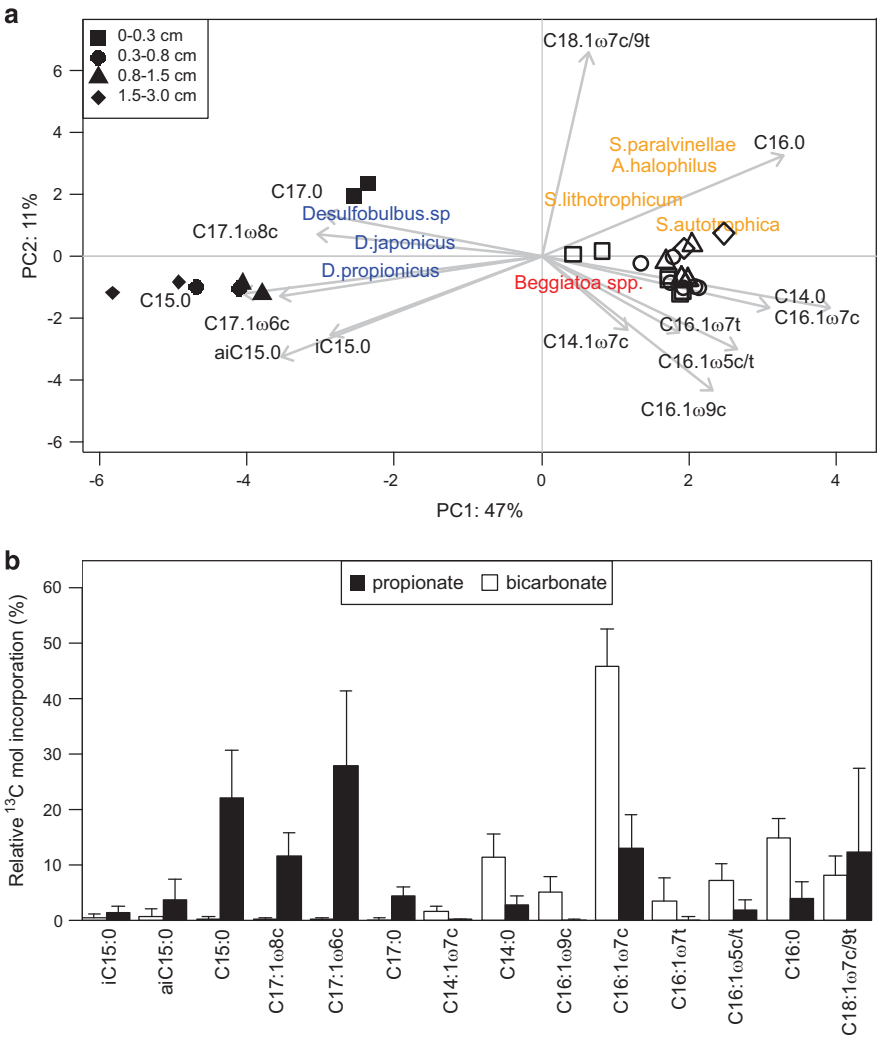

Figure 2 (**a**) Principal component analysis (PCA) of ^{13}C-substrate incorporation (pmol g^{-1} dry weight) normalized to mol% and log transformed before analysis. The first two axes of the PCA explain 58% of the variance among samples. Grey arrows represent the proportion of total variance explained by each fatty acid. Filled symbols indicate samples treated with ^{13}C-propionate, open symbols are samples treated with ^{13}C-bicarbonate and shapes indicate sediment layers as shown in legend. Only sediment layers with high cable bacteria densities were included in the analysis (see Materials and methods). Reference bacteria were added to PCA: *Desulfobulbus* spp. (blue), sulphur-oxidizing Gammaproteobacteria (red) and sulphur-oxidizing Epsilonproteobacteria (yellow, for references see Materials and methods). (**b**) Average (± s.d.) percent of total ^{13}C-incorporation for each PLFA in all layers included in PCA plot for both substrate additions (black: propionate $n = 8$, white: bicarbonate $n = 20$).

8.4 to 7.8, the oxygen penetration depth doubled (Figure 5b) and the DOU showed an almost fourfold decrease (from 81 ± 2 to 24 ± 13 mmol O_2 m^{-2} day^{-1}). However, after 24 h of incubation, the pH peak (8.3) as well as the DOU (61 ± 5 mmol O_2 m^{-2} day^{-1}) had almost fully re-established. PLFA-SIP analysis showed a negative impact on both carbon assimilation rates, with the strongest inhibition occurring in sediment zones below the cut (Figures 5e and h and Supplementary Figure S3). In particular, propionate consumption decreased by 70% whereas bicarbonate uptake for both March and August experiments decreased on average 48%. However, the overall reduction in carbon uptake was substantially less in the cutting experiments compared with the anoxic treatment (Table 1), and this may indicate a temporal rather than permanent halt of the e-SOx process. In the top oxic layer, propionate assimilation was variable with no change for one replicate and an increase of 45% for the second core; however, mean inorganic carbon fixation was always enhanced in the oxic zone, with an increase of 40% for March and 73% for the August experiment.

When the sediment was cut half way through the suboxic zone (at 0.8 cm), the subsurface pH maximum disappeared and the oxygen consumption decreased dramatically post cut (from 80 ± 20 to 28 ± 6 mmol O_2 m^{-2} day^{-1}, Figure 5c) and both parameters did not recover in the remainder of the experiment. Carbon uptake rates were strongly reduced (>80%) below the cut (Figures 5f and i)

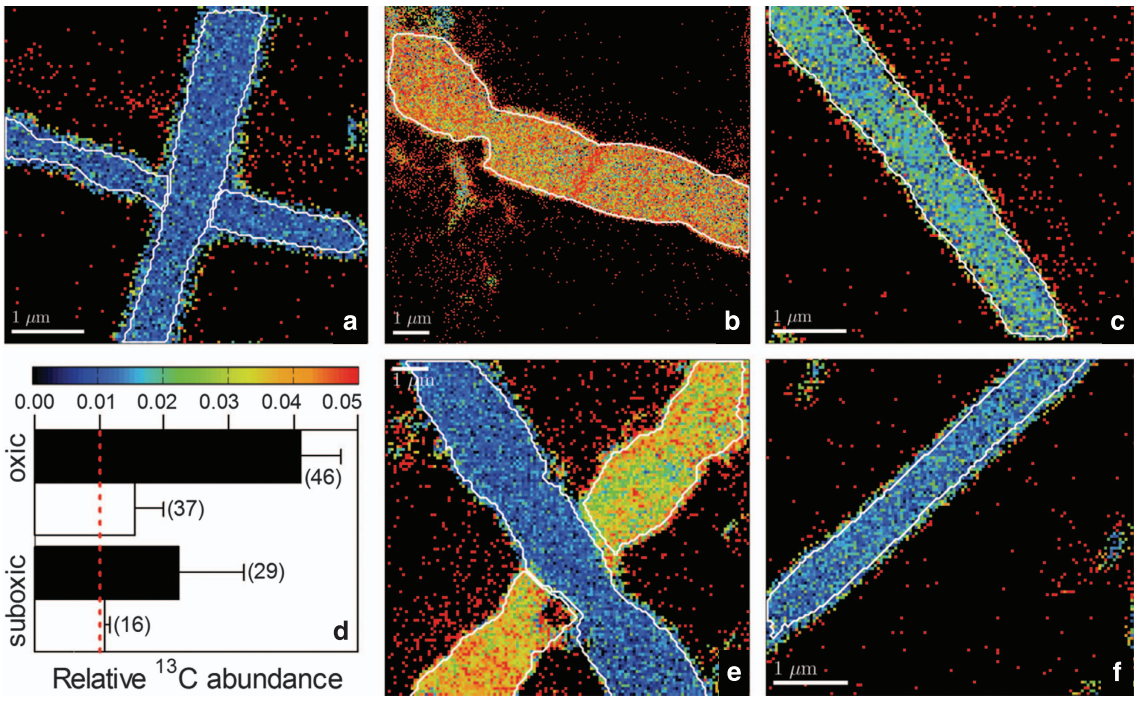

Figure 3 Shown are example images of the relative ^{13}C-abundance ($^{13}C/(^{13}C+^{12}C)$) in individual cable bacteria measured by nanoSIMS: natural ^{13}C-abundance Controls (**a**), ^{13}C-propionate incorporation (**b**, **e**) and ^{13}C-bicarbonate uptake (**c**, **f**). Filaments are outlined in white. Images in top row are from the oxic layer (0–0.2 cm) whereas bottom row images are from the suboxic layer (0.4–2.0 cm). Colour scale shows natural ^{13}C-abundance (0.01) in blue and ^{13}C-enrichment increases towards red (0.05). (**d**) Average (± s.d.) values of relative ^{13}C-abundance in filaments from different sediment layers and for different ^{13}C-labelled substrates (black: propionate, white: bicarbonate) are shown. Red dotted line indicates the value for the Control filaments. Number of cells analysed are in parenthesis.

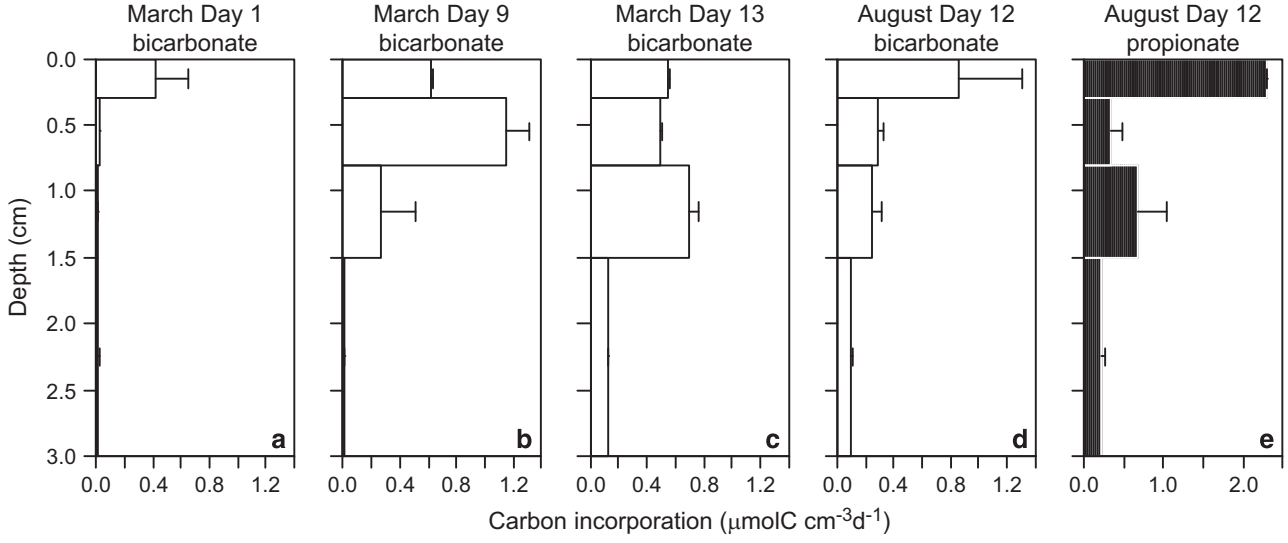

Figure 4 Depth profiles of inorganic carbon incorporation rates in bacterial biomass for March days 1 (**a**), 9 (**b**) and 13 (**c**) and August day 12 (**d**) as well as propionate uptake rates for August day 12 (**e**). Average (± s.d.) rates were calculated from PLFA-SIP labelling, corrected for source labelling levels and converted to total biomass as described in the Materials and methods ($n = 2$).

with values comparable to those obtained for the anoxic treatment. Propionate uptake was not substantially altered above the cutting depth, but bicarbonate incorporation was somewhat inhibited in the suboxic layer directly above the cut and again stimulated in the top layer. The combined results, from all three manipulation experiments, suggest that both inorganic and organic carbon assimilation were tightly linked with the e-SOx process.

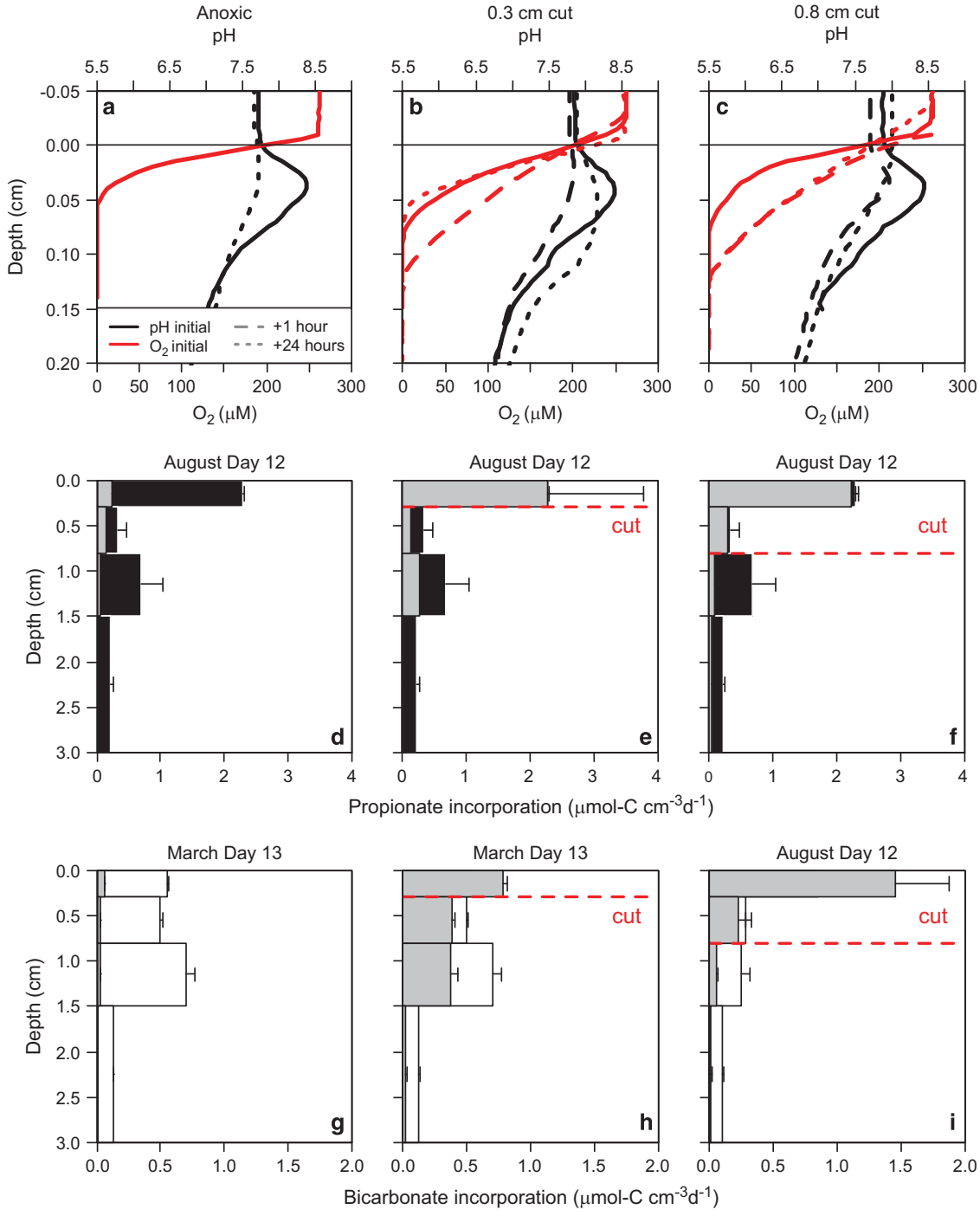

Figure 5 Effects of manipulation experiments on microsensor profiles and carbon incorporation in sediment with fully developed geochemical fingerprint of the e-SOx process. Left column shows effects of anoxia, middle column corresponds to the 0.3 cm deep cut and right column indicates results from the deeper 0.8 cm cut. Top row shows microsensor profiles of oxygen (red) and pH (black) for starting conditions, and hours after manipulation are indicated in the legend. Only one representative replicate per treatment is shown for clarity ($n = 3$); other replicates were similar. Carbon incorporation rates as calculated from ^{13}C-PLFA analysis are represented in bar plots (**d–i**) with unmanipulated sediment in black (propionate) or white (bicarbonate) and rates obtained 24 h after sediment were manipulated in grey. Averages (± s.d.) are plotted. Number of replicate cores was 2. Results of the shallow cut (0.3 cm deep) for August day 12 experiment can be found in Supplementary Figure S3.

Discussion

Electrogenic sulphur oxidation

The microsensor and FISH data obtained in our sediment incubations confirmed results obtained in a previous field study (Malkin *et al.,* 2014) and laboratory experiments (Nielsen *et al.,* 2010; Risgaard-Petersen *et al.,* 2012; Schauer *et al.,* 2014). The temporal development of the characteristic geochemical fingerprint of the e-SOx process is

accompanied by the downward growth of a dense network of long filamentous cable bacteria that span the suboxic zone (Malkin *et al.,* 2014; Schauer *et al.,* 2014). Cable bacteria densities at peak development were half of those recorded in a similar sediment incubation experiment (2380 m cm^{-2}, Schauer *et al.,* 2014) but three- to sixfold higher than densities in the suboxic zone (0.3–0.8 cm) observed under field conditions (120 m cm^{-3}, Malkin *et al.,* 2014). In addition, we estimate that e-SOx was responsible for ~70% of the sedimentary oxygen consumption given the steep increase in DOU from days 6 to 13 and the sharp decrease in DOU 1 h after cutting the sediment. This estimate closely aligns with the contribution of 81% found by Schauer *et al.* (2014) and highlights the important role that e-SOx can play in sedimentary geochemical cycling. The drastic geochemical effects observed in the manipulation experiments, with either induced anoxia or cutting of the sediment at 0.3 cm depth, were consistent with previous observations (Nielsen *et al.,* 2010; Pfeffer *et al.,* 2012) and confirm the current conceptual model of e-SOx in which electrons are transported from anodic cells to cathodic cells along the longitudinal axis of cable bacteria filaments.

Carbon metabolism and growth of cable bacteria

We used two ^{13}C-stable isotope approaches (PLFA-SIP and nanoSIMS) to study the carbon metabolism of the fast-growing cable bacteria. PLFA-SIP identified high incorporation of propionate in 15:0, 17:1ω6c and 17:1ω8c fatty acids that we attributed to be biomarkers for cable bacteria given that those resemble the fatty acid composition of *Desulfobulbus* spp. (Taylor and Parkes, 1983; Pagani *et al.,* 2011) to which cable bacteria are most closely related (Pfeffer *et al.,* 2012; Malkin *et al.,* 2014). Propionate is steadily produced through mineralization of organic matter in sediments and serves as a major energy and carbon source for several Deltaproteobacteria (Sorensen *et al.,* 1981; Parkes *et al.,* 1989; Purdy *et al.,* 1997). Rates of propionate assimilation measured with PLFA-SIP (17 mmol C m^{-2} day^{-1}) scale well with biomass accruement of the cable bacteria based on FISH counts (16 mmol C m^{-2} day^{-1}), suggesting that cable bacteria could successfully grow on propionate in the environment. Moreover, based on ^{13}C-dissolved inorganic carbon measurements obtained from pore water, we estimated that only 2% of the propionate assimilated was respired, indicating that propionate was mainly used as a carbon source by the cable bacteria rather than being respired by sulphate-reducing bacteria. However, we found that propionate incorporation (7 mmol C m^{-2} day^{-1}) estimated by nanoSIMS explained 44% of the observed biomass increase (FISH). *Desulfobulbus* spp. can also grow on lactate, acetate, ethanol, propanol and pyruvate (Laanbroek and Pfennig, 1981; Widdel and Pfennig, 1982; Parkes *et al.,* 1993; Pagani *et al.,* 2011), and therefore it seems plausible that cable bacteria use other organic substrates besides propionate.

An autotrophic metabolism is unlikely as the biomass increase calculated from ^{13}C-inorganic carbon uptake (nanoSIMS) only explains ~15% of the observed cable bacteria growth. The limited incorporation of ^{13}C-bicarbonate measured in cable bacteria (~20% of propionate uptake) is well within the range observed in heterotrophic microorganisms (Roslev *et al.,* 2004; Hesselsoe *et al.,* 2005; Wegener *et al.,* 2012) and inorganic incorporation can therefore most likely be attributed to anapleurotic reactions.

The fast expansion of the cable bacteria filament network, as observed in our incubations, has been previously explained by an exponential growth mechanism with high generation times, and continuous and uniform cell divisions throughout the filament (Schauer *et al.,* 2014). When generation time is calculated based on ^{13}C-propionate incorporation (nanoSIMS) and FISH counts (using the same assumptions as Schauer *et al.,* 2014 for the filament density at day 0), this provides the short generation time (20 h) previously reported by Schauer *et al.* (2014). However, our ^{13}C-propionate incorporation (nanoSIMS) results indicate that the turnover of cathodic, oxygen-respiring cells is twice as fast as that of anodic, sulphide-oxidizing cells. This suggests different energy yields from each half redox reactions that lead to rapid-growing cathodic cells and less-efficient anodic cells. Moreover, estimation of growth efficiencies calculated from biomass increase (16 mmol C m^{-2} day^{-1}) and COC (54 mmol O_2 m^{-2} day^{-1}) suggest an efficiency of 30%. Previously, a ratio of 1:1 of oxygen to carbon was reported for the cable bacteria (Schauer *et al.,* 2014), but our results reveal higher energy dissipation from the transport of electrons along the cm-long filament. The metabolic differences between spatially and temporally distinct cable bacterial populations highlight the need for pure cultures to further study the growth characteristics of this recently discovered bacterium.

As observed previously (Pfeffer *et al.,* 2012), the cutting manipulation at 0.3 cm had an immediate and drastic response in the geochemistry of the sediment, suggesting an instant arrestment of e-SOx, presumably because of physical disruption of the electron transport by the cable bacteria filaments. Our manipulation experiments however indicate that under some conditions, this impediment of e-SOx may not be permanent. Unlike the cutting experiment of Pfeffer *et al.* (2012), we observed a partial restoration of the e-SOx geochemical signature 24 h after the cut at 0.3 cm. Cable bacteria filament network below the cut (which were no longer in contact with oxygen) managed to regain or maintain part of their suboxic carbon uptake activity that was substantially higher than in the anoxic treatment. The treatment with the deeper cutting

depth at 0.8 cm did not show any sign of recovery of e-SOx activity after 24 h. These distinct effects between the two cutting depths at 0.3 and 0.8 cm suggest that the recovery potential of the cable bacteria network depends on the location of disturbance with a critical threshold of a couple of mm within 24 h. Re-establishment of e-SOx activity after cutting could be explained by fast regrowth at the upper terminal end of the cable filament, or perhaps, by reorientation, implying some form of motility as proposed by Schauer *et al.* (2014). The mechanism by which the transport of electrons is re-established requires further study into chemotactic and motility capacities of the cable bacteria.

Associated chemoautotrophic community

Intriguingly, high rates of inorganic carbon fixation were measured in this study in concert with the downward development of the heterotrophic cable bacteria. Total inorganic carbon assimilation was sixfold higher than those reported for subtidal environments (Enoksson and Samuelsson, 1987; Thomsen and Kristensen, 1997) and sandy intertidal sediments (Lenk *et al.,* 2011) but are well within the range of rates obtained in sulphidic salt-marsh creek sediments (Boschker *et al.,* 2014). Although inorganic carbon fixation was high in horizons dominated by e-SOx, this inorganic carbon is unlikely assimilated by the cable bacteria themselves, but rather by other chemoautotrophic bacteria. Clone libraries revealed that sulphur-oxidizing Epsilon- and Gammaproteobacteria were not only present in the oxic zone, but persisted throughout the suboxic zone. PLFA analysis with ^{13}C-bicarbonate labelling also provided a biomarker fingerprint that was consistent with chemoautotrophic sulphur-oxidizing Epsilon- and Gammaproteobacteria (Inagaki *et al.,* 2003; Takai *et al.,* 2006; Li *et al.,* 2007; Glaubitz *et al.,* 2009; Sorokin *et al.,* 2010; Labrenz *et al.,* 2013). Hence, both clone libraries and PLFA-SIP suggest that sulphur-oxidizing bacteria from the Epsilon- and Gammaproteobacteria may be the main chemoautotrophic organisms in sediments with e-SOx. The difference in depth distribution of inorganic carbon incorporation between the March and August experiments might be related to the initial conditions in the seasonal hypoxic Marine Lake Grevelingen, where bottom waters were oxic in March (80% O_2 saturation) as opposed to anoxic in August (0% O_2 saturation). To conclude, the presence of the cable bacteria performing e-SOx process favoured the codevelopment of a strongly active chemoautotrophic community that extends down to cm of depth in the sediment.

Manipulation experiments provided further evidence of a tight coupling between subsurface chemoautotrophic organisms and the electron transport by the cable filament network. Induced anoxia demonstrated that chemoautotrophs in the suboxic zone directly depend on the oxygen in the overlying water given the almost complete inhibition of ^{13}C-bicarbonate uptake throughout the sediment. Similarly, inorganic carbon incorporation drastically decreased below the cutting depth (in the 0.8 cm cutting depth treatment) and was only maintained in sediment layers where cable bacteria were still connected to oxygen. Inorganic carbon fixation was actually stimulated in the surface sediment layer after cutting, and this could be because of an increased potential for reoxidation after doubling in oxygen penetration once the cable network was disrupted. Finally, when the sediment was cut at 0.3 cm depth, bicarbonate uptake only slightly decreased (still maintained 50 to 70% of initial activity) as did propionate uptake by the cable bacteria, suggesting that chemoautotrophs partially recovered in synchrony with the re-establishment of the e-SOx process after 24 h.

Our study therefore suggests that the complete oxidation of sulphide in e-SOx sediments may be a two-step process, regulated by a consortium of bacteria composed of chemoorganotrophic cable bacteria and sulphur-oxidizing chemolithoautotrophs, rather than by the cable bacteria alone. Given that in the deeper layers, oxygen and nitrate are absent (Risgaard-Petersen *et al.,* 2012; Marzocchi *et al.,* 2014) chemolithoautotrophs have to use other electron acceptors to oxidize reduced sulphur compounds. Although these chemolithoautotrophs may disproportionate sulphur (Grote *et al.,* 2012; Wright *et al.,* 2013), their metabolic link to the cable bacteria indicates they use the cable bacteria possibly as an electron sink by tapping on to the electron transport network via nanowires, nanotubes or fimbrae (Widdel and Pfennig, 1982; Reguera *et al.,* 2005; Dubey and Ben-Yehuda, 2011). Clearly, further studies are needed to confirm key autotrophic players and to target the exact mechanisms by which the observed activity of the chemolithoautotrophic bacteria is coupled to the electron transport network of the cable bacteria. Our results suggest that other bacteria may benefit directly from the electron transport by the cable bacteria.

Conflict of Interest

The authors declare no conflict of interest.

Acknowledgements

We thankfully acknowledge the assistance with stable isotope analysis by Peter van Breugel and Marco Houtekamer, Michiel Kienhuis for technical assistance with nanoSIMS analysis, molecular work of Bekir Faydaci and Sinem Atli and the help of Anton Tramper and Pieter van Rijswijk during sediment collection. This work was financially supported by the Darwin Centre for Geoscience (to HTSB and FJRM), ERC grant to FJRM, Danish Council for Independent Research-Natural Sciences (to RS), The Netherlands Earth System Science Centre (to JJM) and an NWO large infrastructure subsidy to JJM.

References

Boschker HTS, Nold SC, Wellsbury P, D Bos, W de Graaf, R Pel *et al.* (1998). Direct linking of microbial populations to specific biogeochemical processes by ^{13}C-labelling of biomarkers. *Nature* **392**: 801–805.

Boschker HTS, Middelburg JJ. (2002). Stable isotopes and biomarkers in microbial ecology. *FEMS Microbiol Ecol* **40**: 85–95.

Boschker HTS, Vasquez-Cardenas D, Bolhuis H, Moerdijk-Poortvliet TWC, Moodley L. (2014). Chemoautotrophic carbon fixation rates and active bacterial communities in intertidal marine sediments. *PLoS One* **9**: e101443.

Brinch-Iversen J, King GM. (1990). Effects of substrate concentration, growth-state, and oxygen availability on relationships among bacterial carbon, nitrogen and phospholipid phosphorus-content. *FEMS Microbiol Ecol* **74**: 345–355.

Dannenberg S, Kroder M, Dilling W, Cypionka H. (1992). Oxidation of H_2, organic compounds and inorganic sulphur compounds coupled to reduction of O_2 or nitrate by sulphate-reducing bacteria. *Microbiology* **158**: 93–99.

Donachie SP, Bowman JP, On SLW, Alam M. (2005). *Arcobacter halophilus* sp. nov., the first obligate halophile in the genus Arcobacter. *Int J Syst Evol Microbiol* **55**: 1271–1277.

Dubey GP, Ben-Yehuda S. (2011). Intercellular nanotubes mediate bacterial communication. *Cell* **144**: 590–600.

Enoksson V, Samuelsson M. (1987). Nitrification and dissimilatory ammonium production and their effects on nitrogen flux over the sediment-water interface in bioturbated coastal sediments. *Mar Ecol Prog Ser* **36**: 181–189.

Fuseler K, Cypionka H. (1995). Elemental sulphur as an intermediate of sulphide oxidation with oxygen by *Desulfobulbus propionicus*. *Arch Microbiol* **164**: 104–109.

Glaubitz S, Lueders T, Abraham W-R, Jost G, Jürgens K, Labrenz M. (2009). ^{13}C-isotope analyses reveal that chemolithoautotrophic Gamma- and Epsilonproteobacteria feed a microbial food web in a pelagic redoxcline of the central Baltic Sea. *Environ Microbiol* **11**: 326–337.

Grote J, Schott T, Bruckner CG, Glöckner FO, Jost G, Teeling H *et al.* (2012). Genome and physiology of a model Epsilonproteobacterium responsible for sulphide detoxification in marine oxygen depletion zones. *Proc Natl Acad Sci USA* **109**: 506–510.

Guckert JB, Antworth CP, Nichols PD, White DC. (1985). Phospholipid, ester-linked fatty-acid profiles as reproducible assays for changes in prokaryotic community structure of estuarine sediments. *FEMS Microbiol Ecol* **31**: 147–158.

Hesselsoe M, Nielsen JL, Roslev P, Nielsen PH. (2005). Isotope labelling and microautoradiography of active heterotrophic bacteria on the basis of assimilation of $^{14}CO_2$ isotope labelling and microautoradiography of active heterotrophic bacteria on the basis of assimilation of $^{14}CO_2$. *Appl Environ Microbiol* **71**: 646–655.

Inagaki F, Takai K, Kobayashi H, Nealson K, Horikoshi K. (2003). *Sulfurimonas autotrophica* gen. nov., sp. nov., a novel sulphur-oxidizing Epsilonproteobacterium isolated from hydrothermal sediments in the Mid-Okinawa Trough. *Int J Syst Evol Microbiol* **53**: 1801–1805.

Inagaki F, Takai K, Nealson KH, Horikoshi K. (2004). *Sulfurovum lithotrophicum* gen. nov., sp. nov., a novel sulphur-oxidizing chemolithoautotroph within the Epsilonproteobacteria isolated from Okinawa Trough hydrothermal sediments. *Int J Syst Evol Microbiol* **54**: 1477–1482.

Jørgensen BB. (1978). Comparison of methods for the quantification of bacterial sulphate reduction in coastal marine-sediments 1. Measurement with radiotracer techniques. *Geomicrobiol J* **1**: 11–27.

Laanbroek HJ, Pfennig N. (1981). Oxidation of short-chain fatty acids by sulphate-reducing bacteria in freshwater and in marine sediments. *Arch Microbiol* **128**: 330–335.

Labrenz M, Grote J, Mammitzsch K, Boschker HTS, Laue M, Jost G *et al.* (2013). *Sulfurimonas gotlandica* sp. nov., a chemoautotrophic and psychrotolerant Epsilonproteobacterium isolated from a pelagic redoxcline, and an emended description of the genus *Sulfurimonas*. *Int J Syst Evol Microbiol* **63**: 4141–4148.

Lenk S, Arnds J, Zerjatke K, Musat N, Amann R, Mußmann M. (2011). Novel groups of Gammaproteobacteria catalyse sulphur oxidation and carbon fixation in a coastal intertidal sediment. *Environ Microbiol* **13**: 758–774.

Li Y, Peacock A, White D, Geyer R, Zhang C. (2007). Spatial patterns of bacterial signature biomarkers in marine sediments of the Gulf of Mexico. *Chem Geol* **238**: 168–179.

Malkin SY, Rao AM, Seitaj D, Vasquez-Cardenas D, Zetsche E-M, Hidalgo-Martinez S *et al.* (2014). Natural occurrence of microbial sulphur oxidation by long-range electron transport in the seafloor. *ISME J* **8**: 1843–1854.

Manz W, Amann R, Ludwig W, Wagner M, Schleifer KH. (1992). Phylogenetic oligodeoxynucleotide probes for the major subclasses of proteobacteria - problems and solutions. *Syst Appl Microbiol* **15**: 593–600.

Marzocchi U, Trojan D, Larsen S, Louise Meyer R, Peter Revsbech N, Schramm A *et al.* (2014). Electric coupling between distant nitrate reduction and sulphide oxidation in marine sediment. *ISME J* **8**: 1682–1690.

Middelburg JJ, Barranguet C, Boschker HTS, Herman PMJ, Moens T, Heip CHR. (2000). The fate of intertidal microphytobenthos carbon: an in situ 13C-labeling study. *Limnol Oceanogr* **45**: 1224–1234.

Nielsen LP, Risgaard-Petersen N, Fossing H, Christensen PB, Sayama M. (2010). Electric currents couple spatially separated biogeochemical processes in marine sediment. *Nature* **463**: 1071–1074.

Pagani I, Lapidus A, Nolan M, Lucas S, Hammon N, Deshpande S *et al.* (2011). Complete genome sequence of *Desulfobulbus propionicus* type strain (1pr3). *Stand Genomic Sci* **4**: 100–110.

Parkes RJ, Gibson GR, Mueller-Harvey I, Buckingham WJ, Herbert RA. (1989). Determination of the substrates for sulphate-reducing bacteria within marine and estuarine sediments with different rates of sulphate reduction. *J Gen Microbiol* **135**: 175–187.

Parkes RJ, Dowling NJE, White D, Herbert R, Gibson G. (1993). Characterization of sulphate-reducing bacterial populations with marine and estuarine sediments with different rates of sulphate reduction. *FEMS Microbiol. Ecol.* **102**: 235–250.

Pfeffer C, Larsen S, Song J, Dong M, Besenbacher F, Meyer RL *et al.* (2012). Filamentous bacteria transport electrons over centimetre distances. *Nature* **491**: 218–221.

Purdy KJ, Nedwll DB, Embley TM, Takii S. (1997). Use of 16S rRNA-targeted oligonucleotide probes to investigate the occurrence and selection of sulfate-reducing bacteria in response to nutrient addtion to sediment slurry microcosms from a Japanesse estuary. *FEMS Microbiol Ecol* **24**: 221–234.

Reguera G, McCarthy KD, Mehta T, Nicoll JS, Tuominen MT, Lovley DR. (2005). Extracellular electron transfer via microbial nanowires. *Nature* **435**: 1098–1101.

Risgaard-Petersen N, Revil A, Meister P, Nielsen LP. (2012). Sulphur, iron-, and calcium cycling associated with natural electric currents running through marine sediment. *Geochim Cosmochim Acta* **92**: 1–13.

Romanova ND, Sazhina F. (2010). Relationships between the cell volume and the carbon content of bacteria. *Oceanology* **50**: 522–530.

Roslev P, Larsen M, Jorgensen D, Hesselsoe M. (2004). Use of heterotrophic CO_2 assimilation as a measure of metabolic activity in planktonic and sessile bacteria. *J Microbiol Methods* **59**: 381–393.

Schauer R, Risgaard-Petersen N, Kjeldsen KU, Tataru Bjerg JJ, B Jørgensen B, Schramm A *et al.* (2014). Succession of cable bacteria and electric currents in marine sediment. *ISME J* **8**: 1314–1322.

Sorokin DY, Kovaleva OL, Tourova TP, Muyzer G. (2010). *Thiohalobacter thiocyanaticus* gen. nov., sp. nov., a moderately halophilic, sulphur-oxidizing gammaproteobacterium from hypersaline lakes, that utilizes thiocyanate. *Int J Syst Evol Microbiol* **60**: 444–450.

Sorensen J, Christensen D, Jorgensen BB. (1981). Volatile fatty acids and hydrogen as substrates for sulfate-reducing bacteria in anaerobic marine sediment. *Appl Environ Microbiol* **42**: 5–11.

Takai K, Suzuki M, Nakagawa S, Miyazaki M, Suzuki Y, Inagaki F *et al.* (2006). *Sulfurimonas paralvinellae* sp. nov., a novel mesophilic, hydrogen- and sulphur-oxidizing chemolithoautotroph within the Epsilonproteobacteria isolated from a deep-sea hydrothermal vent polychaete nest, reclassification of *Thiomicrospira denitrificans* as *Sulfurimonas denitrificans* comb. nov. and emended description of the genus *Sulfurimonas*. *Int J Syst Evol Microbiol* **56**: 1725–1733.

Taylor J, Parkes RJ. (1983). The cellular fatty acids of the sulphate-reducing bacteria, *Desulfobacter* sp., *Desulfobulbus* sp. and *Desulfovibrio desulfuricans*. *J Gen Microbiol* **129**: 3303–3309.

Thomsen U, Kristensen E. (1997). Dynamics of sum CO_2 in a surficial sandy marine sediment: the role of chemoautotrophy. *Aquat Microb Ecol* **12**: 165–176.

Wegener G, Bausch M, Holler T, Thang NM, Mollar XP, Kellermann MY *et al.* (2012). Assessing sub-seafloor microbial activity by combined stable isotope probing with deuterated water and 13C-bicarbonate. *Environ Microbiol* **14**: 1517–1527.

Widdel F, Pfennig N. (1982). Studies on dissimilatory sulphate-reducing bacteria that decompose fatty acids. II. Incomplete oxidation of propionate by Desulfobulbus propionicus gen. nov., sp. nov. *Arch Microbiol* **131**: 360–365.

Wright KE, Williamson C, Grasby SE, Spear JR, Templeton AS. (2013). Metagenomic evidence for sulphur lithotrophy by Epsilonproteobacteria as the major energy source for primary productivity in a sub-aerial arctic glacial deposit. *Borup Fiord Pass Front Microbiol* **4**: 63.

Zhang CL, Huang Z, Cantu J, Pancost RD, Brigmon RL, Lyons TW *et al.* (2005). Lipid biomarkers and carbon isotope signatures of a microbial (*Beggiatoa*) mat associated with gas hydrates in the Gulf of Mexico. *Appl Environ Microbiol* **71**: 2106–2112.

Supplementary Information accompanies this paper on The ISME Journal website (http://www.nature.com/ismej)